Nonpyramidal neurons in the primate basolateral amygdala: A Golgi study in the baboon (Papio cynocephalus) and long-tailed macaque (Macaca fascicularis)

2 authors:

Alexander Joseph Mcdonald
University of South Carolina
100 PUBLICATIONS   9,432 CITATIONS

James R Augustine
University of South Carolina
24 PUBLICATIONS   2,422 CITATIONS

Some of the authors of this publication are also working on these related projects:

Project   Muscarinic Modulation of the Basolateral Amygdala View project

RESEARCH ARTICLE

JCN RESEARCH IN SYSTEMS NEUROSCIENCE
THE JOURNAL OF COMPARATIVE NEUROLOGY

WILEY

Nonpyramidal neurons in the primate basolateral amygdala: A Golgi study in the baboon (*Papio cynocephalus*) and long-tailed macaque (*Macaca fascicularis*)

Alexander J. McDonald ⓘ | James R. Augustine

Department of Pharmacology, Physiology and Neuroscience, University of South Carolina School of Medicine, Columbia, South Carolina

Correspondence
Alexander J. McDonald, Department of Pharmacology, Physiology and Neuroscience, University of South Carolina School of Medicine, Columbia, SC 29208.
Email: alexander.mcdonald@uscmed.sc.edu

Abstract

Nonpyramidal GABAergic interneurons in the basolateral nuclear complex (BNC) of the amygdala are critical for the regulation of emotion. Remarkably, there have been no Golgi studies of these neurons in nonhuman primates. Therefore, in the present study we investigated the morphology of nonpyramidal neurons (NPNs) in the BNC of the baboon and monkey using the Golgi technique. NPNs were scattered throughout all nuclei of the BNC and had aspiny or spine-sparse dendrites. NPNs were morphologically heterogeneous and could be divided into small, medium, large, and giant types based on the size of their somata. NPNs could be further divided on the basis of their somatodendritic morphology into four types: multipolar, bitufted, bipolar, and irregular. NPN axons, when stained, formed dense local arborizations that overlapped their dendritic fields to varying extents. These axons always exhibited varying numbers of varicosities representing axon terminals. Three specialized NPN subtypes were recognized because of their unique anatomical features: axo-axonic cells, neurogliaform cells, and giant cells. The axons of axo-axonic cells formed "axonal cartridges," with clustered varicosities that contacted the axon initial segments of pyramidal neurons (PNs). Neurogliaform cells had small somata and numerous short dendrites that formed a dense dendritic arborization; they also exhibited a very dense axonal arborization that overlapped the dendritic field. Giant cells had very large irregular somata and long, thick dendrites; their distal dendrites often branched extensively and had long appendages. In general, the NPNs of the baboon and monkey BNC, including the specialized subtypes, were similar to those of rodents.

KEYWORDS

axo-axonic cell, basolateral amygdala, chandelier cell, Golgi technique, interneurons, neurogliaform cell, primates

1 | INTRODUCTION

The basolateral nuclear complex (BNC) of the amygdala is a critical hub in forebrain circuits regulating emotional behavior and emotional memory. The main cell types in the BNC mediating projections to other forebrain regions are glutamatergic neurons with pyramidal or semi-pyramidal somata and spiny dendrites. These neurons are often termed pyramidal neurons (PNs) because of their resemblance to cortical pyramidal cells (McDonald, 1992; Millhouse & DeOlmos, 1983). Like the cortex, the BNC also contains a variety of interneuronal GABAergic nonpyramidal neurons (NPNs) with aspiny or sparsely-spiny dendrites that tightly regulate the firing of PNs (Capogna, 2014;

McDonald, 1992, 2019; Spampanato, Polepalli, & Sah, 2011; Veres, Nagy, & Hájos, 2017; Veres, Nagy, Vereczki, Andrási, & Hájos, 2014).

NPN subpopulations with distinct morphological characteristics were originally described in Golgi preparations in rodents and other nonprimate species (Hall, 1972; Kamal & Tömböl, 1975; McDonald, 1982, 1984; McDonald & Culberson, 1981; Millhouse & DeOlmos, 1983; Mukhina & Leontovich, 1970; Tömböl & Szafrańska-Kosmal, 1972). Subsequent immunohistochemical studies in rodents demonstrated that NPNs with different neurochemical signatures exhibited distinctive innervation patterns in relation to separate PN compartments and/or other NPNs (Bienvenu, Busti, Magill, Ferraguti, & Capogna, 2012; Capogna, 2014; McDonald, 2019; Muller, Mascagni, & McDonald, 2003, 2005, 2006, 2007; Rhomberg et al., 2018; Vereczki et al., 2016). For example, rodent NPNs that express the calcium-binding protein parvalbumin (PV) or the neuropeptide cholecystokinin (CCK) mainly innervate the perisomatic compartment of pyramidal cells where they can control PN spiking (Muller et al., 2006; Vereczki et al., 2016; Veres et al., 2014, 2017), whereas those that express somatostatin (SOM) mainly innervate the distal dendritic compartment of PNs where they can regulate synaptic plasticity involved in emotional learning by shunting excitatory inputs (Capogna, 2014; Muller et al., 2007; Wolff et al., 2014). GABAergic interneurons also control oscillatory activity in the rodent BNC, which has been shown to be critical for synaptic plasticity involved in fear learning and extinction in rodents (Capogna, 2014; Pape and Paré, 2010). Because disruption in GABAergic inhibition in the BNC in humans produces hyperexcitability which results in increases in anxiety, emotional dysregulation, and seizure activity (Prager, Bergstrom, Wynn, & Braga, 2016), it is critical to analyze the structure and function of GABAergic NPNs in the primate BNC. Moreover, comparisons of inhibitory systems of primates and rodents will be necessary to determine if data on GABAergic mechanisms gleaned from studies in rodents also apply to the BNC of human and nonhuman primates.

Although there have been fewer immunohistochemical studies of NPN subpopulations in human and nonhuman primates, for the most part similar subpopulations appear to exist in these species as well. Thus, BNC NPNs in monkey are GABAergic (McDonald & Augustine, 1993; Pitkänen & Amaral, 1994), and separate subpopulations in monkeys and humans express PV (Mascagni, Muly, Rainnie, & McDonald, 2009; Pitkänen & Amaral, 1993a; Sorvari et al., 1995) or SOM (Amaral, Avendaño, & Benoit, 1989; Desjardins & Parent, 1992; Mascagni et al., 2009; McDonald, Mascagni, & Augustine, 1995). Remarkably, although there have been two Golgi studies of the BNC in humans (Braak & Braak, 1983; Tosevski et al., 2002), and two Golgi studies of PNs in monkeys (Herzog, 1982; Morgan & Amaral, 2014), there have been no studies of BNC NPNs in nonhuman primates using the Golgi technique.

Golgi techniques can provide morphological information about all parts of *individual* impregnated neurons: somata, dendrites, and axons. Immunohistochemical studies typically stain somatodendritic and axonal compartments separately, but rarely allow the entire extent of individual neurons to be appreciated. In addition, the Golgi technique potentially permits the visualization of neurons that do not express any of the neurochemical markers currently used to identify NPN subpopulations. Intracellular filling of neurons also affords complete staining of individual neurons but has the disadvantage that each cell is filled individually, as opposed to Golgi techniques where thousands of cells are visualized in one preparation. In the present study, the rapid Golgi technique was used to stain NPNs in baboons (*Papio cynocephalus)* and long-tailed macaques (*Macaca fascicularis)*. Morphological heterogeneity was observed in somata, dendrites, and local axonal arborizations of NPNs in both species.

2 | MATERIALS AND METHODS

2.1 | Animals

Four adult male savanna baboons (*Papio cynocephalus*; obtained from the Southwest National Primate Research Center, Southwest Foundation for Biomedical Research, San Antonio, Texas) and two adult male macaques (*Macaca fascicularis*; obtained from Upjohn, Kalamazoo, Michigan) were used in this study. The macaques had been used previously by Upjohn for blood pressure studies. Both sets of animals were housed in the Animal Research Facility on the School of Medicine Campus of the University of South Carolina. Their housing and care followed the NIH "Guide for the Care and Use of Laboratory Animals". Veterinary care was available at all times.

2.2 | Tissue processing

Vascular perfusion-fixation was carried out under deep anesthesia using ketamine hydrochloride (I.P, Veterinary Products, Bristol Laboratories, Division of Bristol-Myers, Syracuse, NY) supplemented with sodium pentobarbital (I.V.; Veterinary Laboratories, Lenexa, KS) (Augustine & White, 1986). The descending aorta was clamped and the animals were perfused using a gravity perfusion method (Cox, Heys, & Heys, 1977). Following an initial wash with 0.1 M phosphate-buffered saline (PBS) at room temperature for 30 s, the animals were perfused with 4 L of Sorensen's phosphate-buffered 4% glutaraldehyde-0.5% paraformaldehyde (for baboons) or 4% paraformaldehyde (for macaques) at room temperature delivered over a 30 min interval. The brains were removed and postfixed for 6 hr at 4°C in the perfusate. Amygdalas were excised, sliced into 5-mm blocks, and impregnated using a modification of the rapid Golgi technique (Lund, 1973). After impregnation, blocks were encased in a shell of paraffin (Fox, Ubeda-Purliss, Ihrig, & Biagioli, 1951) and sectioned at 150 μm in the coronal plane. Every fifth section, however, was cut at 50–75 μm and stained with cresyl violet to aid in determining the location of Golgi-impregnated neurons in surrounding thick sections. The thick sections (150 μm) were collected between sheets of filter paper in 100% alcohol, cleared in xylene, mounted on glass slides, and coverslipped with Permount (Fisher Scientific, West Columbia, SC). The thin sections (50–75 μm) were collected in 100% alcohol in ice cube tray cubicles with perforated bottoms. While in the ice cube tray cubicles, sections were hydrated in descending alcohols, stained with

cresyl violet, dehydrated in ascending alcohols, cleared in xylene, mounted on glass slides, and coverslipped with Permount.

2.3 | Analysis

Sections were analyzed using an Olympus BX51 microscope (Tokyo, Japan). Digital light micrographs were taken with an Olympus DP2-BSW camera system. NPNs were identified on the basis of exhibiting aspiny or spine-sparse dendrites. In contrast, dendrites of PNs were densely-spiny. The location of all neurons was determined using the descriptions and photographs of BNC nuclei in the long-tailed macaque (*Macaca fascicularis*) provided by Amaral and co-workers (1992) (Figure 1). The cytoarchitecture of the BNC in Nissl-stained preparations of baboons and macaques appeared identical. The same nuclear subdivisions were present and their shapes and relative proportions were the same in both species, although the baboon BNC was slightly larger than that of the macaque. All drawings of Golgi-impregnated NPNs were made with a 100X oil-immersion objective and a drawing tube. A calibrated ocular reticule was used to measure the widths of dendrites, diameters of axonal varicosities, lengths of axonal cartridges of axo-axonic cells, and the lengths and widths of NPN somata. The sum of the lengths and widths of somata was used as a measure of somatic size. Axo-axonic cells in the present

FIGURE 1 Coronal Nissl-stained section through the amygdala of the macaque monkey. Nuclei of the monkey amygdala (nomenclature of Amaral, Price, Pitkanen, & Carmichael, 1992): ABmc, magnocellular accessary basal nucleus; ABpc, parvicellular accessary basal nucleus; ABvm, ventromedial accessary basal nucleus; Bi, intermediate basal nucleus; Bmc, magnocellular basal nucleus; Bpc, parvicellular basal nucleus; CL, lateral central nucleus; CM, medial central nucleus; Ldm, dorsomedial lateral nucleus; Lvl, ventrolateral lateral nucleus; M, medial nucleus; PAC, periamygdaloid cortex; PL, paralaminar nucleus. Scale bar = 750 μm [Color figure can be viewed at wileyonlinelibrary.com]

study formed "axonal cartridges" containing clustered axonal varicosities; we measured the length of 20 randomly selected cartridges in the baboon accessory basal nucleus, where they were most commonly seen, and counted the numbers of varicosities seen in each cartridge.

3 | RESULTS

3.1 | General characteristics and classification of BNC NPNs based on differences in somatic size and shape

Golgi-stained neurons in the BNC of both primate species were similar. The great majority of Golgi-stained neurons were PNs with very spiny dendrites (Figure 2a). NPNs, exhibiting aspiny, or spine-sparse dendrites (Figure 2b), were observed in the BNC of all brains, but were more common in the baboon BNC. In addition, the morphology of NPNs were easier to examine in the baboon because the staining was less dense. Therefore, most of the drawings and photographs of NPNs in this article are from the BNC of the baboon. In both species, small numbers of NPNs were seen in all of the BNC nuclei where they appeared to be scattered randomly throughout each nucleus.

NPNs in the primate BNC were morphologically heterogeneous. For the most part, BNC NPNs appeared to constitute a continuous morphological spectrum in regard to somatic, dendritic, and axonal anatomy. However, three "specialized" subtypes could be identified on the basis of unique anatomical features: (a) axo-axonic (chandelier) cells; (b) neurogliaform cells; and (c) giant cells. We will first describe the general somatic, dendritic, and axonal features of NPNs and then describe the morphology of the three specialized cell types.

The majority of NPNs had somata that were smaller than those of surrounding PNs in all BNC nuclei. For description purposes four classes of NPNs can be distinguished based on differences in the size of their somata (i.e., the sum of the lengths and widths of somata): (a) small (sum of 15–29 μm); (b) medium-sized (sum of 30–39 μm); (c) large (sum of 40–49 μm); and giant (sum of 50–70 μm). NPNs with giant somata also exhibited unique dendritic and axonal morphology; these specialized NPNs are termed "giant cells" in this account. They will be described separately (see below).

The shape of NPN somata was largely determined by the number, thickness, and place of origin of their primary dendrites from the soma. Four types of BNC NPNs were thus distinguished: (a) multipolar; (b) bitufted; (c) bipolar; and (d) irregular. Multipolar NPNs typically had four or more primary dendrites that extended in all directions giving these neurons a stellate appearance (Figures 2b, 3b,c, 4b,c, 6a, 7, 10, 11). Bitufted NPNs had fusiform somata, and most primary dendrites arose from opposite poles of the soma (Figures 3a, 4a, 8, 9). Bipolar NPNs had fusiform somata, and two primary dendrites that arose from opposite poles of the soma (Figure 12). Irregular NPNs, which were mainly giant cells, had somata that were distorted by the presence of a small number of very thick primary dendrites (Figure 16).
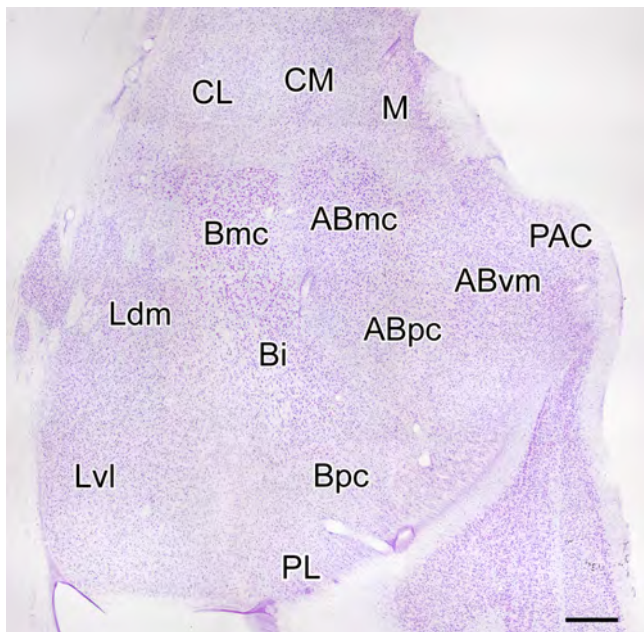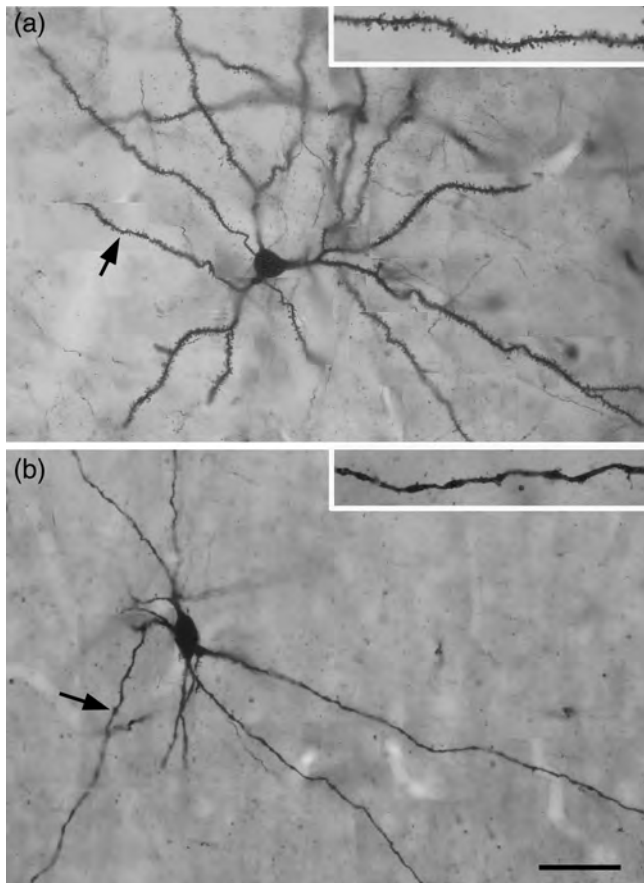
FIGURE 2 Photomontages of a typical PN (a) and NPN (b) in the baboon BNC, showing the differences in dendritic spine densities. (a) PN in the Ldm of the baboon. Arrow points to the dendrite shown at higher power in the inset. Note the high spine density. (b) Large multipolar NPN in the ABmc of the baboon. Arrow points to the dendrite shown at higher power in the inset. Note the low spine density on this varicose dendrite. Scale bar = 50 μm for a and b; insets are at higher power

3.2 | Dendritic morphology of BNC NPNs

The thickness of primary dendrites of NPNs was correlated with somatic size. Small NPNs had primary dendrites that were 1.0–1.5 μm thick (Figures 3c, 4c, 10, 11) whereas medium-sized NPNs had primary dendrites that were 1.5–3.0 μm thick (Figures 3b, 4a, 8, 9). The primary dendrites of most large NPNs were 2–4 μm thick (Figures 2b, 3a, 4b, 7). Secondary dendrites were thinner than primary dendrites. More distal dendrites were usually not significantly thinner than secondary dendrites, but were often varicose (e.g., Figure 2b).

Dendrites of some NPNs had very few if any spines (Figures 3c, 4c, 9–12), but most had a small number of spines randomly distributed along their dendrites and could thus be considered "spine-sparse" (Figures 2b, 3a,b, 4a,b, 7, 8). Most of these spines were short, resembling those of PNs, but some were longer.

Dendrites of most NPNs had 0–3 branch points. The size and shape of dendritic arborizations was often correlated with the size and shape of somata. Multipolar neurons typically had round or ovoid
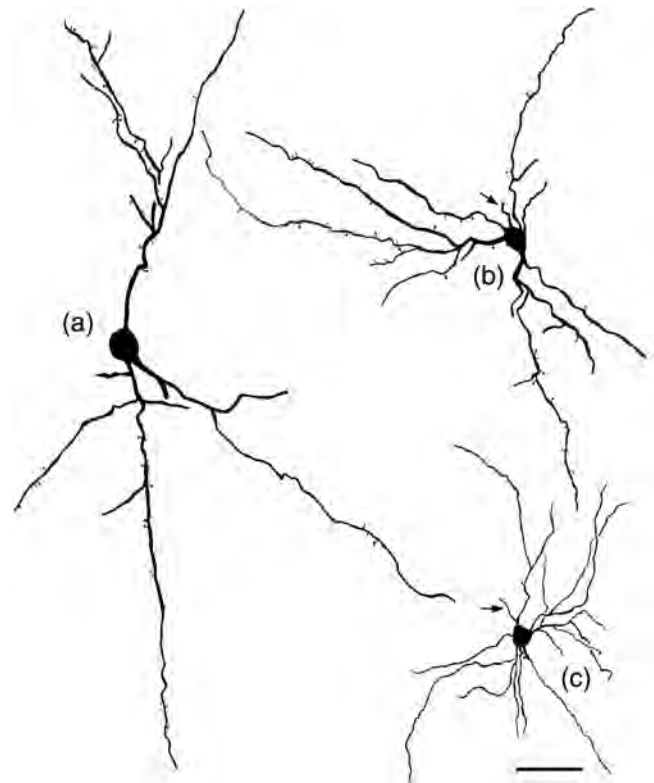

FIGURE 3 Drawings of NPNs selected to illustrate variations in their somatodendritic morphology. Arrows indicate initial portions of the axon. (a) Large bitufted NPN in the Lvl (baboon). Axon was not stained. (b) Medium-sized multipolar NPN in the Bpc (baboon). (c) Small multipolar NPN in the ABmc (baboon). Scale bar = 50 μm

dendritic fields. Dendritic fields of most small multipolar NPNs were usually about 200–250 μm in diameter (e.g., Figures 3c, 4c, 10, 11) whereas large multipolar NPNs had dendritic arborizations that were often over 500 μm in diameter. Bipolar and bitufted NPNs typically had dendritic fields that were elliptical and could measure up to 500–600 μm long and 250–300 μm wide (Figures 3a, 4a, 8, 9, 12)

Two separate varicose dendrites of one NPN in the baboon Lvl formed a series of intimate dendrodendritic contacts with varicose distal dendrites of two other NPNs whose somata were not in the same section (Figure 5). In both cases, the dendrites made a series of contacts within a span of 20 μm. In the case illustrated in Figure 5 the dendrite on the left was a distal dendrite of the neuron whose soma was contained in the section; the dendrite on the right was the distal tip of the other dendrite and it terminated at the point shown in the photomicrograph. The other dendrite of the neuron whose soma was in the section had a similar series of contacts onto the initial portion of a secondary dendrite whose origin from its primary dendrite was only 20 μm from its soma.

3.3 | Axonal morphology of BNC NPNs

Axons of BNC NPNs usually originated from somata, but occasionally from primary dendrites. Although axons of some NPNs were not stained (Figures 3a, 4a,b), the majority of NPNs exhibited axonal staining.
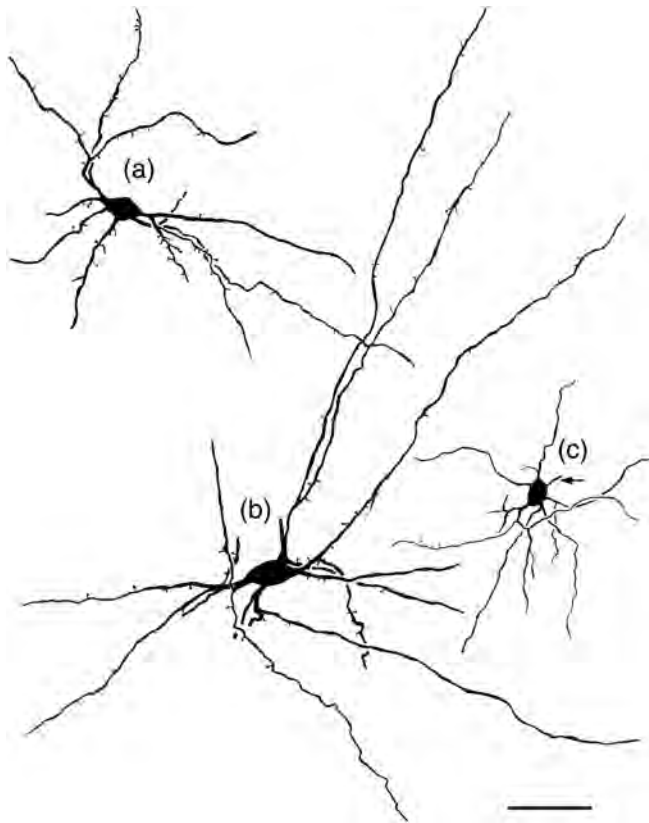
FIGURE 4 Drawings of NPNs selected to illustrate variations in their somatodendritic morphology. Arrows indicate initial portions of the axon. (a) Medium-sized bitufted NPN in the Bmc (baboon). Axon was not stained. (b) Large multipolar NPN in the ABmc (baboon). Axon was not stained. (c) Small multipolar NPN in the Bmc (macaque). Scale bar = 50 μm
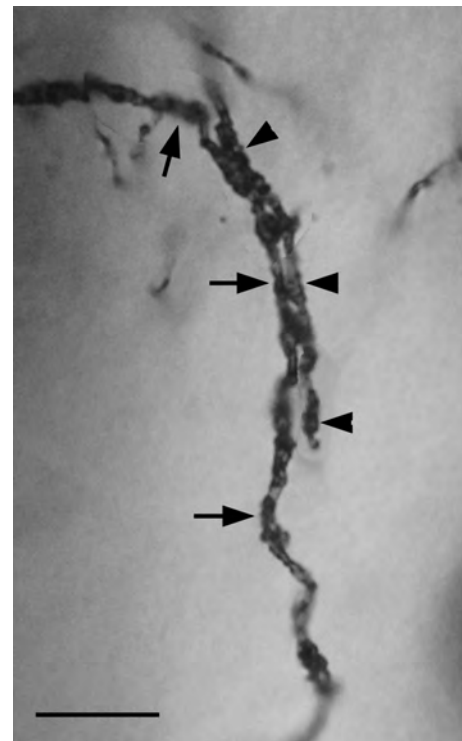

FIGURE 5 Photomontage of dendrodendritic contacts between dendrites of two different NPNs in the Lvl nucleus (baboon). The dendrite indicated by arrows arose from a medium-sized multipolar NPN whose soma was in this section. The dendrite indicated by arrowheads arose from a soma in an adjacent section. A different dendrite of this same multipolar NPN exhibited similar contacts with another NPN dendrite. Scale bar = 10 μm

Most axons were 1–2 μm thick at their origin and gave rise to several fairly thick branches (ca. 1.0 μm thick) near the cell body. These secondary branches gave off many fine collaterals that branched extensively. Most of these axonal arborizations appeared to be fairly extensive but were often difficult to follow and draw because of dense axonal staining of other neurons in the vicinity. The axons of 8 NPNs were relatively isolated from surrounding staining and could be accurately drawn (Figures 6–14). The axonal arborizations of some NPNs virtually completely overlapped their dendritic arborizations (Figures 7, 11), while those of others were confined to one side (Figures 8–10).

Axonal branches of all NPNs exhibited variable numbers of varicosities, most likely corresponding to axon terminals, that varied in size depending on the neuron. Axons of some NPNs had relatively small varicosities (1.0–1.5 μm in diameter) whereas others had larger varicosities (up to 2.5 μm in diameter). In some neurons the varicosities tended to be clustered (Figures 7, 8, 12).

3.4 | Axo-axonic cells

The axons of axo-axonic cells (AACs) formed "axonal cartridges" that contacted the axon initial segments (AISs) of PNs (Figure 6b, 12, 13).

Axonal cartridges are short segments of axons (ca. 20–30 μm long) that are dominated by a high density of large varicosities (Figure 13). The mean length of 20 randomly selected cartridges in the baboon accessory basal nucleus was 24.90 μm ± 1.18 (Mean ± SEM). In many cases the axon forming the cartridge folded back upon itself, or gave off a branch that was restricted to the cartridge, thus increasing the number of varicosities contained in the cartridge (Figure 13a, b). Axonal cartridges of BNC AACs typically contained 9–16 varicosities (13.35 ± 1.07; Mean ± SEM; n = 20). It is well established from Golgi studies (McDonald & Culberson, 1981) and ultrastructural immuno-histochemical studies (Bienvenu et al., 2012; Muller et al., 2006) in nonprimate species that the varicosities of axonal cartridges of BNC AACs are axon terminals forming symmetrical synapses with AISs of BNC PNs. In our preparations, it was rare to observe axonal cartridges contacting AISs since that requires the staining of both the AAC axon and the postsynaptic PN (Figure 13d). Only two completely stained AACs (i.e., with axons seen arising from somata) were seen in this study (one of these is seen in Figures 6b and 12), and both were observed in the baboon accessory basal nucleus (one in ABvm and one in ABmc). However, isolated axons (i.e., not continuous with their soma of origin) forming axonal cartridges were seen in all nuclei of the BNC, but were especially numerous in the accessory basal nuclei.
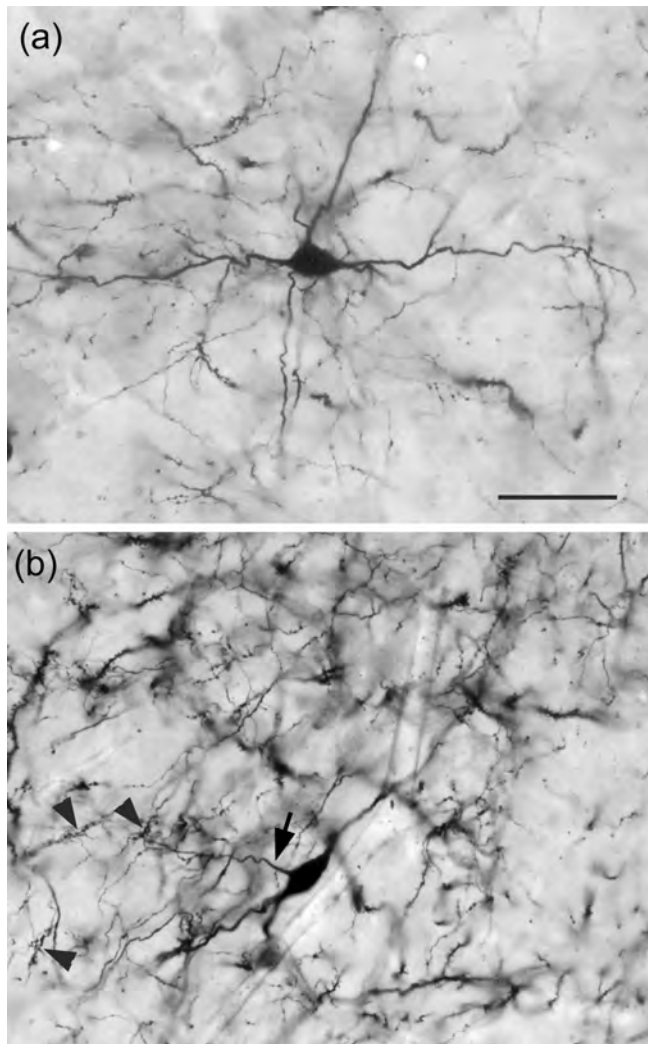
FIGURE 6 Photomicrographs of two NPNs that had easily traceable axons that were drawn using a drawing tube. (a) Large multipolar NPN in the ABmc (baboon; see Figure 7 for drawing). The initial portion of its axon was out of the focal plane of this photomicrograph. (b) Medium-sized bipolar axo-axonic cell in the ABvm (baboon; see Figure 12 for drawing). Arrow indicates the initial portion of the axon. Arrowheads indicate three representative axonal cartridges. Scale bar = 50 μm for both a and b

FIGURE 7 Large multipolar NPN in the ABmc (baboon). Soma and dendrites are black; axon is red. Arrow indicates the initial portion of the axon. Note that the axonal arborization is aligned with the dendritic arborization. The axonal varicosities are 1.0–2.5 μm in diameter and tend to be clustered. This axon made intimate contacts with many spiny dendrites of neighboring PNs. Scale bar = 50 μm [Color figure can be viewed at wileyonlinelibrary.com]

3.5 | Neurogliaform cells

NGFCs are characterized by small somata (8–13 μm in diameter) and many (at least 6) short tortuous dendrites that branch sparingly and have few spines (Figures 14 and 15). The dendritic arborizations are less than 200 μm in diameter. They often appear to form contacts with the spiny dendrites of PNs. The distal dendrites of some of these neurons were thin and beaded, resembling axons (Figure 14B). When observed, the axons arise from somata or the proximal portions of primary dendrites and branch extensively within the field of the dendritic arborization. One NGFC appeared to have two axons. Axonal varicosities were numerous and small (0.5–1.0 μm in diameter). NGFCs were found in small numbers throug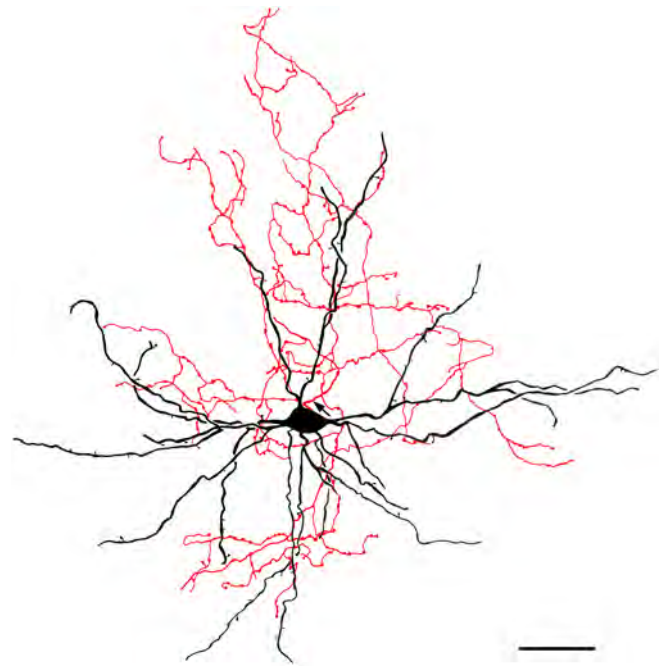hout the BNC of both baboons and macaques. However, in one macaque brain there were 15 NGFCs in the Lvl in just two sections; there was no axonal or dendritic overlap between these 15 cells.

3.6 | Giant cells

Giant cells are the NPNs with the largest somata (Figure 16). The sum of the lengths and widths of these somata were 47–70 μm. Somata were typically irregular in shape because they were distorted by giving rise to 2–3 primary dendrites that were very thick (3–7 μm). Dendrites often branched extensively, especially near their terminations, and commonly extended for over 400 μm. Distal dendrites sometimes gave rise to many spines, some of which were very long (Figures 16 and 17). Spines on more proximal dendrites were short and sparse. Only the initial portions of the axons (first 20–35 μm) were ever stained. Most giant cells were seen in the lateral and accessory basal nuclei.

4 | DISCUSSION

This is the first study to investigate the morphology of NPNs in the BNC of nonhuman primates using the Golgi technique. These neurons were identified by the presence of aspiny or spine-sparse dendrites. They were randomly scattered throughout all BNC nuclei but were greatly outnumbered in each nucleus by spine-dense PNs. NPNs were

FIGURE 8 Medium-sized bitufted NPN in the Bpc (baboon). Soma and dendrites are black; axon is red. Arrow indicates the initial portion of the axon. The axonal arborization is located along the right side of the neuron. Its varicosities are 1.0–1.5 μm in diameter. Scale bar = 50 μm [Color figure can be viewed at wileyonlinelibrary.com]

FIGURE 9 Medium-sized bitufted NPN in the paralaminar nucleus (baboon). Soma and dendrites are black; axon is red. Arrow indicates the initial portion of the axon. The axonal arborization is located along the lower part of the neuron. Its varicosities are 1.0–1.5 μm in diameter. Scale bar = 50 μm [Color figure can be viewed at wileyonlinelibrary.com]

morphologically heterogeneous. For the most part, BNC NPNs appeared to constitute a continuous morphological spectrum in regard to somatic, dendritic, and axonal anatomy. Their somata were usually smaller than those of neighboring PNs, but some were as large, or even larger, than PNs. The dendrites of most NPNs had only a small number of branches, but the axons of most NPNs, when stained, typically formed dense local arborizations typical of interneurons. Three "specialized" subtypes could be identified on the basis of unique anatomical features: (a) axo-axonic (chandelier) cells; (b) neurogliaform cells; and (c) giant cells. As discussed below, the morphology of NPNs in the primate BNC, including the specialized subtypes, are very similar to those of rodents. This suggests that electrophysiological and behavioral findings in rodents can probably be extrapolated to NPNs of nonhuman primates and humans.

4.1 | Comparisons with Golgi studies in other species

There have been two Golgi studies of BNC NPNs in humans (Braak & Braak, 1983; Tosevski et al., 2002). As in the nonhuman primate BNC, Braak and Braak (1983) described spiny "class 1" neurons as well as NPNs (class II neurons) in the human amygdala. The latter closely resembled the generalized (i.e., "nonspecialized") NPNs seen in the present study. As in the baboon and monkey, the morphology of the

somata and dendrites of these class II neurons varied greatly. Although some contained lipofuschin granules and some did not, the overall morphology of both types was similar. Unfortunately the axons of these cells were not stained. The Braaks also described somewhat smaller lipofuschin-negative neurons with short dendrites and an axon that arborized modestly near the soma. It was suggested that these "class III" neurons might correspond to the neurogliaform neurons seen in nonprimates. However, most of these cells had only 4–6 dendrites and somata that could be as large as 20 μm in diameter, suggesting that they most likely correspond to the small non-NGF NPNs seen in the present study rather than the NPNs we termed NGFCs. Tosevski et al. (2002) described two types of spiny neurons (Types 1 and 2) as well as aspiny or spine-sparse (Type 3) neurons in the human BNC. Like the NPNs in the present study these Type 3 neurons in the human BNC were "morphologically heterogeneous" and had axons that "ramified considerably," although no drawings or photographs documented the extent and density of these arborizations. Their Type 3 neurons included a subclass of "gliaform" neurons that appear to correspond to the NGFCs of the present study. They had small spherical somata (9 × 7 μm), 5–9 spine-sparse dendrites that were short and profusely branched, and dense local axonal arborizations. Neither AACs nor their axonal cartridges have been seen in Golgi studies of the human BNC. However, axonal cartridges have been observed in light and electron microscopic immunohistochemical

FIGURE 10 Small multipolar NPN in the Lvl (baboon). Soma and dendrites are black; axon is red. Arrow indicates the initial portion of the axon. There are very few well developed varicosities and most are small (1.0 μm). Scale bar = 50 μm [Color figure can be viewed at wileyonlinelibrary.com]

FIGURE 11 Small multipolar NPN in the Lvl (baboon). Soma and dendrites are black; axon is red. Arrow indicates the initial portion of the axon. The axonal arborization is aligned with the dendritic arborization. The axonal varicosities are 1.0–2.0 μm in diameter and tend to be clustered. The axon appeared to make contacts with several spiny dendrites of neighboring PNs. Scale bar = 50 μm [Color figure can be viewed at wileyonlinelibrary.com]

FIGURE 12 Medium-sized bipolar chandelier cell in the ABvm (baboon). Soma and dendrites are black; axon is red. Arrow indicates the initial portion of the axon. Note that the axon exhibits many cartridges, some of which are indicated by arrowheads. Scale bar = 50 μm [Color figure can be viewed at wileyonlinelibrary.com]

studies of the human BNC using antibodies to PV (Sorvari, Soininen, Paljärvi, Karkola, & Pitkänen, 1995). The failure to observe AACs in the human BNC in Golgi-stained preparations is undoubtedly related to the well-established selectivity and capriciousness of staining with this technique (Morest, 1981).

There have been Golgi studies in a wide variety of nonprimate species including the dog, cat, opossum, rabbit, fox, pig, and several rodent species (Hall, 1972; Kamal & Tömböl, 1975; McDonald, 1982, 1984; McDonald & Culberson, 1981; Millhouse & DeOlmos, 1983; Mukhina & Leontovich, 1970; Równiak, Szteyn, & Robak, 2003; Tömböl & Szafrańska-Kosmal, 1972). In all of these species there are scattered aspiny or spine-sparse NPNs in the BNC with dense local axonal arborizations that exhibit considerable morphological diversity, and these are greatly outnumbered by densely-spiny PNs. However, axo-axonic NPNs (AACs) and their axonal cartridges were only observed in previous Golgi studies in the opossum (McDonald & Culberson, 1981) and rat (McDonald, 1982). Given that AACs are present in diverse species, such as the opossum, rat, and baboon, it seems likely that the failure to stain them in all species is due to the capriciousness of the Golgi stain rather than their absence in other species. In the opossum and rat BNC the simple axonal cartridges were called "axonal clusters" because of their clustered varicosities, and the more complex cartridges were termed "axonal nests." These BNC NPNs were termed "amygdaloid chandelier cells" in these earlier studies and
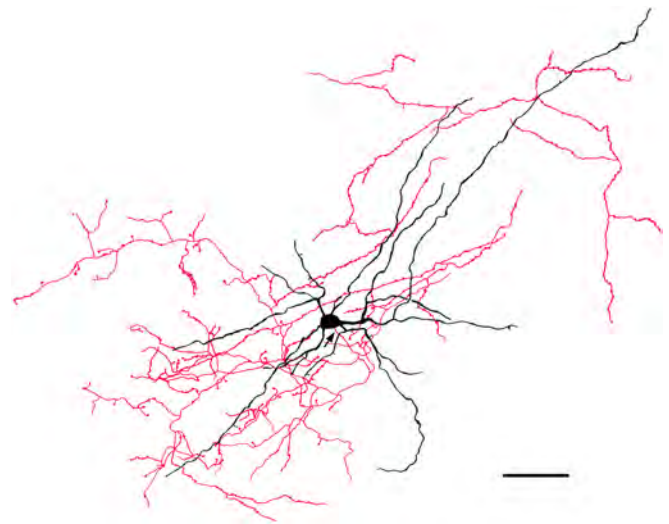
are identical to the AACs seen in primates in the present study. As in the present study in primates, contacts of axonal varicosities of AAC cartridges with the initial segments of PN axons was observed in the opossum and rat (McDonald, 1982; McDonald & Culberson, 1981).
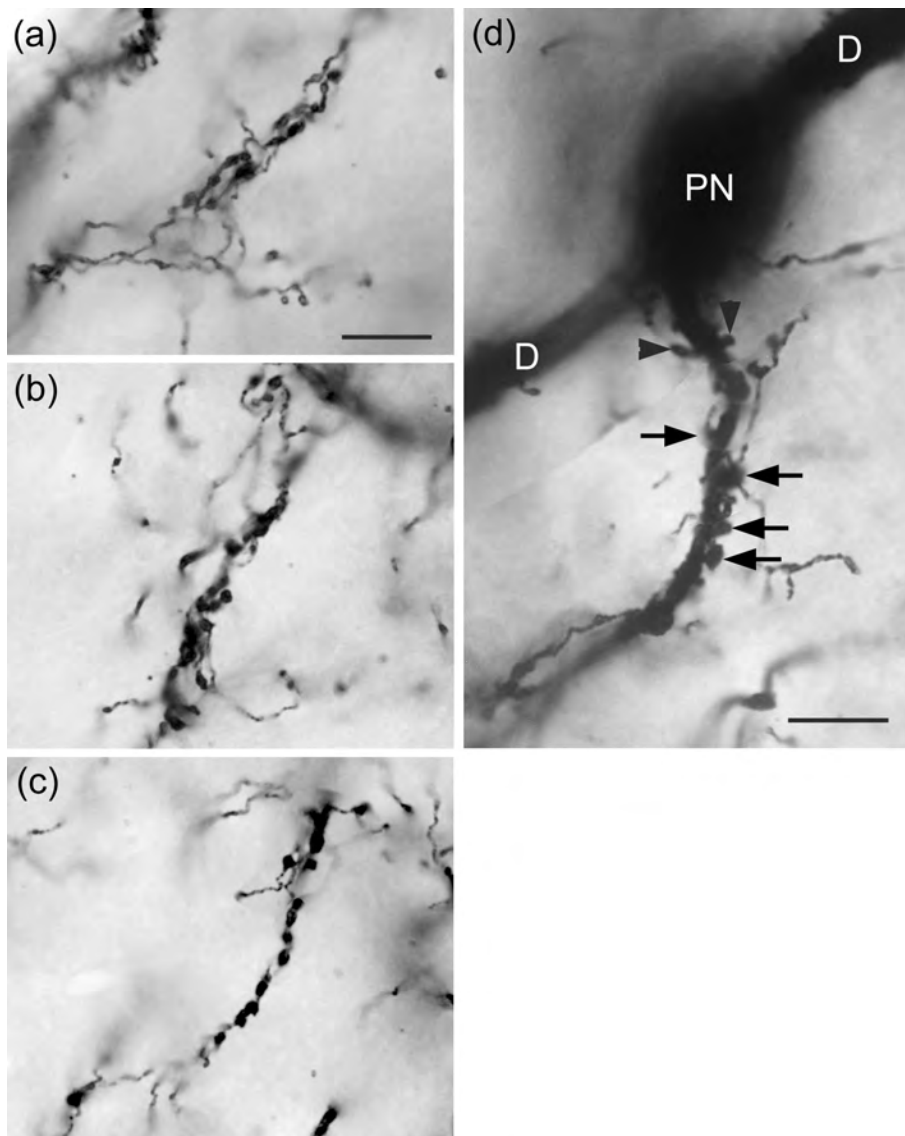
FIGURE 13 Photomontages of axonal cartridges formed by axo-axonic cells in the ABvm (baboon). (a) and (b) complex axonal cartridges exhibiting multiple strands adorned with varicosities. (c) Simple axonal cartridge exhibiting a series of varicosities. (d) Photomontage showing a soma of a PN in the ABmc (PN) giving rise to two primary dendrites (D) (all of which are out of focus in this photomicrograph), and a vertically oriented axon initial segment contacted by an axonal cartridge of an axo-axonic cell. Several varicosities contacting the axon are indicated by unlabeled arrows. Arrowheads indicate spines on the initial segment of the axon of the PN. Scale bar in (a) = 10 μm [(b) and (c) are at the same magnification]. Scale bar in (d) = 10 μm

Chandelier cells were first described in the cerebral cortex where the axon initial segments of cortical PNs (and the axonal cartridges contacting them) are all parallel to each other, thus giving the axonal arborization of these NPNs the appearance of the candlesticks of a chandelier (Fairén & Valverde, 1980; Somogyi, 1977). Since this parallel arrangement of PN axon initial segments is not found in the BNC of any species, the axonal cartridges of BNC axo-axonic chandelier cells are randomly oriented (Figure 12). In the opossum and rat, as in the primate BNC in the present study, the great majority of axons forming cartridges cannot be traced back to their soma of origin. There is evidence in the opossum that the axons of AACs may be myelinated a short distance from their initial segments (McDonald & Culberson, 1981). Since myelin is known to prevent the staining of axons of NPNs in the neocortex (Peters & Proskauer, 1980), this may be the reason that the presumably unmyelinated distal portion of axons that form cartridges usually cannot be followed to their somata of origin. This may also explain why many NPNs with well-impregnated somata and dendrites in the present study did not exhibit significant axonal staining.

Neurogliaform cells (NGFCs) similar to those seen in the primate BNC in the present study closely resemble those seen in previous Golgi studies of the cat (Kamal & Tömböl, 1975; Tömböl & Szafrańska-Kosmal, 1972), opossum (McDonald & Culberson, 1981), rat (McDonald, 1982), human (Tosevski et al., 2002), and several other nonprimate mammals (Równiak et al., 2003). In all species, they have small somata and a large number of short, varicose, spine-sparse dendrites that are very thin. Dendrites of NGFCs in the BNC of primates in the present study often contacted the spiny dendrites of PNs. This was also seen in the opossum (see Figure 8 of McDonald & Culberson, 1981) and rat (see Figs. 19 and 20 of McDonald, 1982). When stained, the axon forms a very dense local arborization that is largely confined to the small spherical dendritic field of the cell. One very interesting aspect of these neurons is that although individual isolated NGFCs were seen throughout the BNC of both the baboon and macaque BNC, 15 of them were concentrated in two sections of the Lvl in one of the macaque brains. This clustering of NGFCs is also seen Golgi preparations of the cat BNC where they were often found in pairs

FIGURE 14 Two neurogliaform cells (NGFCs) in the LvI (macaque). Soma and dendrites are black; axon is red. Arrows indicates the initial portions of the axons. The axonal and dendritic arborizations are more extensive in a than in b. Scale bar = 50 μm [Color figure can be viewed at wileyonlinelibrary.com]
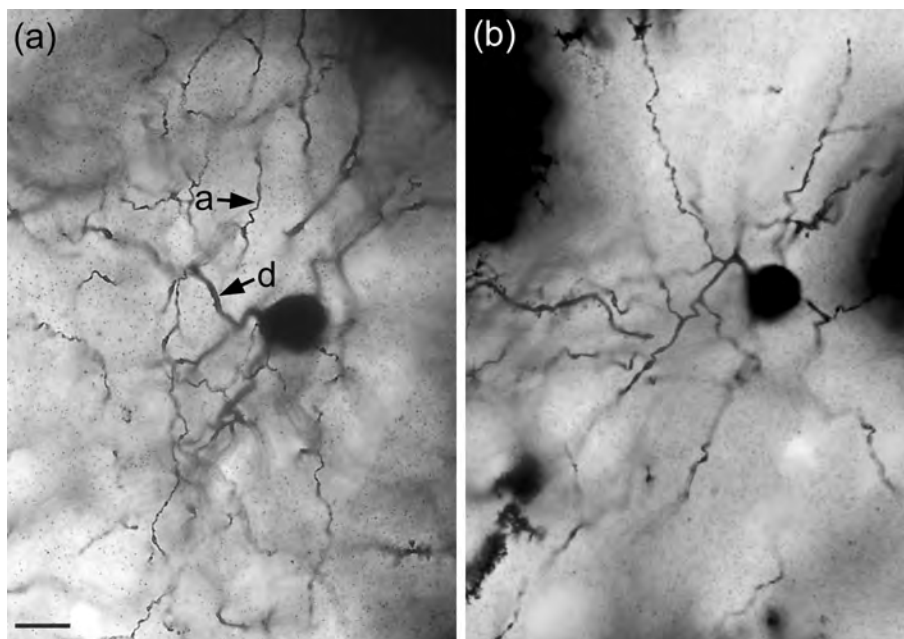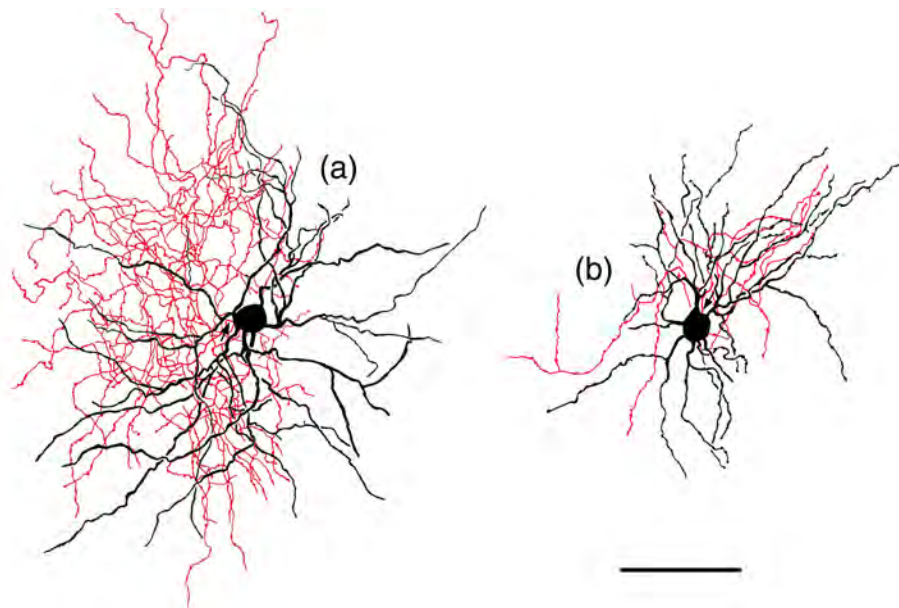

FIGURE 15 Photomicrographs of two NGFCs in the LvI (macaque). (a) Photomicrograph of the NGFC shown in Figure 14a. Segments of dendrites (d) and thinner axons (a) are indicated by arrows. (b) another NGFC that did not have a stained axon. Scale bar = 10 μm for both (a) and (b)

(see Figure 8 of Kamal & Tömböl, 1975). Similarly, only four NGFCs were observed in a Golgi study of the rat brain, but three of these NGFCs were seen in the one brain among the 50 used in the study (McDonald, 1982). Likewise, Golgi-stained NGFCs in the monkey cerebral cortex are often observed in clusters of three or more neurons (Jones, 1975). The reason for this clustering is not clear.

Another distinctive type of NPN seen in the present study were the giant cells. They had very large somata and long, thick dendrites. The distal tips of the dendrites of some of these neurons underwent extensive branching and exhibited numerous dendritic appendages, some of which were very long. Similar dendrites were seen in a Golgi study of the rat BNC (see Figure 8 of McDonald, 1982). Only the initial portion of the axon was stained in all of the giant cells seen in the

present study, which suggests that their axons are myelinated (see above). Interestingly, Millhouse and DeOlmos described neurons that appear to be located in the ventral endopiriform nucleus (although they identified the region as the deep part of the rat piriform cortex) that had very large somata and long, thick dendrites whose distal tips branched extensively and were adorned with numerous long appendages (see Fig. 19 of Millhouse & DeOlmos, 1983). Some of these dendrites remained arborized in the piriform cortex but others extended medially across the external capsule to arborize in the BNC. Just like the giant cells in primates in the present study, only the initial portions of the axons of these cells were stained. Thus, although these very large NPNs in the rat appear to be identical to primate BNC giant cells, they were located in the endopiriform nucleus, just lateral to the
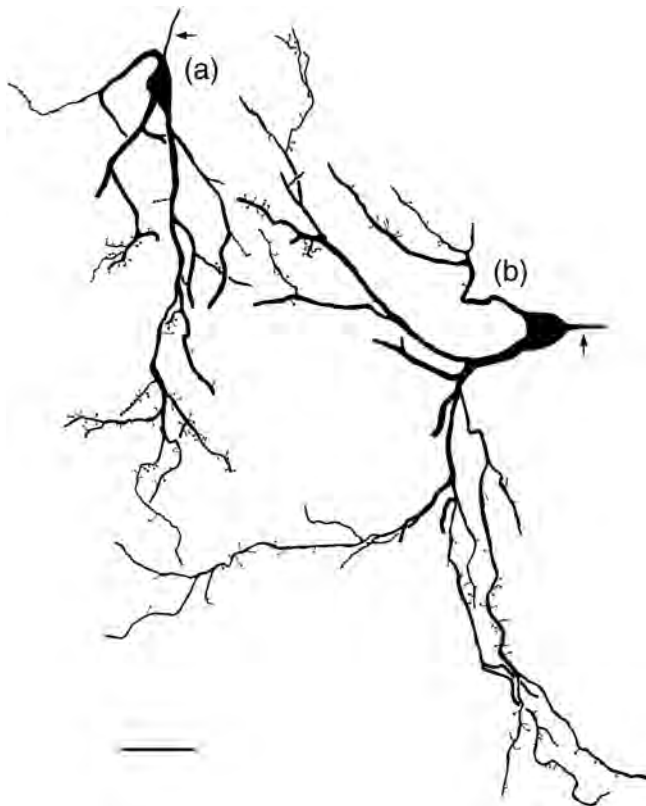
FIGURE 16 Examples of two giant cells. Arrows indicate stained axons; axonal staining ceased within 20–35 of the somata of all giant cells. (a) Giant cell in the Ldm (baboon). (b) Giant cell in the ABmc (baboon). Note that distal dendrites of both neurons exhibit many appendages, some of which are long. Scale bar = 50 μm

FIGURE 17 Photomontage of the dendrite of a giant cell in the Lvm (baboon). Note few dendritic spines on the thick proximal dendrite, but many spines and appendages on its thinner distal dendrites (arrows). Scale bar = 20 μm

BNC. The amygdalar and endopiriform distribution of giant cells, as well as their morphology, strongly suggests that they may correspond to a special population of large NPNs with irregularly-shaped somata located throughout the ventral forebrain that project to the medial portion of the mediodorsal thalamic nucleus (MDm) in rats (McDonald, 1987; Price & Slotnick, 1983) and primates (Russchen, Amaral, & Price, 1987; Timbie & Barbas, 2015). The abrupt termination of Golgi impregnation after the initial segment of their axons, presumably due to myelination, is also more typical of projection neurons than interneurons.

4.2 | Comparisons with immunohistochemical studies in primates and rodents

Immunohistochemical studies of the BNC of all species, including rodents (McDonald, 1985) and primates (McDonald & Augustine, 1993; Pitkänen & Amaral, 1994), indicate that the great majority of NPNs in the BNC, as in the cortex (Kawaguchi & Kubota, 1997), are GABAergic interneurons, although at least some GABAergic NPNs in rats expressing somatostatin, calbindin, or neuropeptide Y are known to project to the basal forebrain or entorhinal cortex (McDonald, Mascagni, & Zaric, 2012; McDonald & Zaric, 2015). Immunohistochemical studies in the rat suggest that the BNC contains at least four
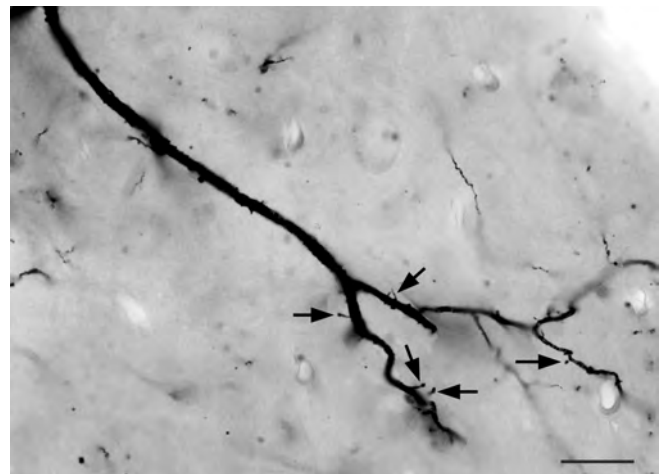
distinct subpopulations of GABAergic NPNs that can be distinguished on the basis of their content of calcium-binding proteins and peptides. These subpopulations are: (a) parvalbumin+/calbindin+ (PV+/CB+) neurons, (b) somatostatin+/calbindin+ (SOM+/CB+) neurons, (c) large multipolar cholecystokinin+ (CCK+) neurons that are often calbindin+ and (d) small bipolar and bitufted interneurons that exhibit extensive colocalization of calretinin (CR), CCK, and vasoactive intestinal peptide (VIP) (Kemppainen & Pitkänen, 2000; Mascagni & McDonald, 2003; McDonald & Betette, 2001; McDonald & Mascagni, 2001, 2002). In addition, a subpopulation of SOM+ neurons, but not other NPN subpopulations, expresses neuropeptide Y (NPY; McDonald, 1989). Interestingly, NPN subpopulations in the rat cortex closely resemble those in the rat BNC, including the two types of CCK+ neurons (Kubota & Kawaguchi, 1994, 1997).

Likewise, immunohistochemical studies of NPNs in the BNC of human and nonhuman primates have shown that subpopulations of these neurons express the calcium-binding proteins PV (Pantazopoulos, Lange, Hassinger, & Berretta, 2006; Pitkänen & Amaral, 1993a; Sorvari et al., 1995), CB (Pantazopoulos et al., 2006; Pitkänen & Amaral, 1993b; Sorvari et al., 1996b) and CR (McDonald, 1994; Sorvari et al., 1996a), as well as the neuropeptides SOM (Amaral et al., 1989; Desjardins & Parent, 1992; McDonald et al., 1995; Schwartzberg, Unger, Weindl, & Lange, 1990), NPY (McDonald et al., 1995; Schwartzberg et al., 1990), and CCK (McDonald & Mascagni, 2019). The same morphological diversity of NPNs seen in the present Golgi study was also observed in the immunohistochemical studies of *each* of these calcium binding proteins and neuropeptides in primates. Thus, immunolabeled NPNs had small, medium-sized, or large somata, and multipolar, bitufted, or bipolar NPNs were observed. There were, however, differences in the percentages of different types of NPNs expressing these markers. For example, in both the monkey (McDonald, 1994) and human BNC (Sorvari et al., 1996a) the majority of CR+ NPNs had small somata. Colocalization studies using

dual-labeling immunohistochemistry have demonstrated that the NPN subpopulations in primates, including humans, are similar, but not identical, to those seen in the rat (Mascagni et al., 2009; Pantazopoulos et al., 2006; Schwartzberg et al., 1990).

There is evidence from light and electron microscopic studies in rodents and primates that different NPN subpopulations have different postsynaptic targets, and thus play specific roles in the circuitry of the BNC (McDonald, 2019). In both rodents (Bienvenu et al., 2012; Vereczki et al., 2016) and primates (Pitkänen & Amaral, 1993a; Sorvari et al., 1995; McDonald & Mascagni, 2019), two separate GABAergic subpopulations, PV+ and CCK+ NPNs, are basket cells that innervate the soma and proximal dendrites of PNs. Remarkably, although a high density of pericellular baskets contacting PN somata are observed in the BNC in immunohistochemical studies of all species studied using antibodies to GABA, PV, or CCK, to the authors' knowledge they have not been described in Golgi studies of the BNC in any species, including the present study. The reason for this is not clear, although there is "a well-known peculiar tendency of the Golgi method to avoid the staining of contiguous structures" (Ramón-Moliner, 1967). The other NPN subpopulation providing perisomatic inputs to BNC PNs are AACs. In nonhuman (Pitkänen & Amaral, 1993a) and human primates (Sorvari et al., 1995), as in rodents (McDonald & Betette, 2001; McDonald & Mascagni, 2001; Veres et al., 2014), the axonal cartridges formed by AACs in the BNC are PV+. In contrast to basket cells, AACs and their axonal cartridges have been observed contacting the axon initial segments of PNs in the BNC of opossum (McDonald & Culberson, 1981) rat (McDonald, 1982) and primates (present study) using the Golgi technique. The use of the Golgi technique has permitted the visualization of the somata, dendrites and axonal arborizations of *individual* AACs, whereas immunohistochemical techniques stain the axonal cartridges but do not permit the identification of the cells of origin of these axons.

In the present study, one Golgi-stained NPN had two of its dendrites contacted by the dendrites of two different NPNs (see Figure 5). These contacts could represent dendrodendritic gap junctions between PV+ NPNs that have been identified in ultrastructural studies of the rat BNC (Muller et al., 2005). Both ultrastructural and electrophysiological studies have shown that the rodent BNC contains a network of PV+ interneurons interconnected by chemical and gap-junctional electrical synapses (Muller et al., 2005; Woodruff & Sah, 2007). Applying a combination of optogenetics, electrophysiology, and high-resolution microscopy allowed Andrási et al. (2017) to demonstrate that actually both PV+ and CCK+ basket cells form separate networks that are interconnected by chemical synapses and gap junctions. However, both types of basket cells synapse with PV+ AACs. Hajos and coworkers conducted quantitative analyses of the innervation of individual PN AISs by AACs in the mouse BNC (Vereczki et al., 2016; Veres et al., 2014). It was found that each AAC in the mouse BNC formed an average of eight contacts with each AIS targeted. Our counts of cartridge varicosities in the baboon BNC were higher (mean of 13). However, this may be due to the fact that better differentiated cartridges were selected for measurement in our study since smaller cartridges with fewer varicosities may not have been recognized as

cartridges, especially because their postsynaptic targets were rarely stained. In the mouse BNC the density of AAC inputs to AISs was highest between 20 and 40 μm of the soma, similar to that seen in the present study (Figure 13), where the threshold for action potential generation was lowest, and where 10–12 AAC synapses, originating from 2 to 3 AACs could block PN firing (Veres et al., 2014). The myelination of AAC axons suggested by Golgi studies should promote near simultaneous release of GABA upon AISs of many PNs, which could be important for the temporal precision of rhythmic oscillations in the BNC. Prominent theta and gamma oscillations occur in the BNC during emotional arousal (Oya, Kawasaki, Howard, & Adolphs, 2002; Paré & Collins, 2000; Paré, Collins, & Pelletier, 2002; Seidenbecher, Laxmi, Stork, & Pape, 2003). These network rhythms are critical for synaptic plasticity associated with the formation and retrieval of emotional memories (Bocchio, Nabavi, & Capogna, 2017; Pape & Paré, 2010; Paré et al., 2002).

Like NGFCs in the cortex (Overstreet-Wadiche & McBain, 2015), NGFCs in the mouse BNC express SOM and NPY (Mańko, Bienvenu, Dalezios, & Capogna, 2012). However, whereas there are some SOM + and NPY+ NPNs in the primate and rat BNC that have small somata typical of NGFCs, the great majority of SOM+ and NPY+ neurons in these species are larger and have fewer and thicker dendrites than the NGFCs seen in Golgi preparations (Amaral et al., 1989; Desjardins & Parent, 1992; McDonald, 1985, 1989; McDonald et al., 1995; Schwartzberg et al., 1990). Therefore, NGFCs appear to be a minority subpopulation of SOM+/NPY+ NPNs in the BNC of these species. The many apparent contacts of NGFC dendrites with PN dendrites suggest the possibility that these cell types many be connected by dendrodendritic gap junctions. NGFCs in the neocortex and hippocampus form electrical synapses mediated by gap junctions with several subtypes of NPNS, including other NGFCs, but not with PNs (Price et al., 2005; Simon, Oláh, Molnár, Szabadics, & Tamás, 2005). It remains to be determined whether gap junctions between NGFCs, or some other common attribute of these neurons, may be responsible for their tendency to occur in clusters in Golgi preparations. Ultrastructural studies of NPY+ NGFCs in the mouse BNC suggest that most of their axon terminals do not form classical synapses, but instead form nonsynaptic appositions with surrounding neurons (Mańko et al., 2012). This is consistent with electrophysiological evidence that NGFCs in the BNC, like those in the neocortex (Overstreet-Wadiche & McBain, 2015), are responsible for a slow GABAergic inhibition mediated by volume transmission (Mańko et al., 2012).

CONFLICT OF INTEREST

The authors state that they have no conflict of interest.

ORCID

Alexander J. McDonald https://orcid.org/0000-0003-3288-9978

REFERENCES

Amaral, D. G., Avendaño, C., & Benoit, R. (1989). Distribution of somatostatin-like immunoreactivity in the monkey amygdala. *The Journal of Comparative Neurology*, *284*, 294–313.

Amaral, D. G., Price, J. L., Pitkanen, A., & Carmichael, S. T. (1992). Anatomical organization of the primate amygdala. In J. P. Aggleton (Ed.), *The Amygdala. Neurobiological aspects of emotion, memory, and mental dysfunction* (pp. 1–66). New York: Wiley-Liss.

Andrási, T., Veres, J. M., Rovira-Esteban, L., Kozma, R., Vikór, A., Gregori, E., & Hájos, N. (2017). Differential excitatory control of 2 parallel basket cell networks in amygdala microcircuits. *PLoS Biology*, *15*, e2001421.

Augustine, J. R., & White, J. F. (1986). The accessory nerve nucleus in the baboon. *The Anatomical Record*, *214*, 312–320.

Bienvenu, T. C., Busti, D., Magill, P. J., Ferraguti, F., & Capogna, M. (2012). Cell-type-specific recruitment of amygdala interneurons to hippocampal theta rhythm and noxious stimuli in vivo. *Neuron*, *74*, 1059–1074.

Bocchio, M., Nabavi, S., & Capogna, M. (2017). Synaptic plasticity, engrams, and network oscillations in amygdala circuits for storage and retrieval of emotional memories. *Neuron*, *94*, 731–743.

Braak, H., & Braak, E. (1983). Neuronal types in the basolateral amygdaloid nuclei of man. *Brain Research Bulletin*, *11*, 349–365.

Capogna, M. (2014). GABAergic cell type diversity in the basolateral amygdala. *Current Opinion in Neurobiology*, *26*, 110–116.

Cox, C. F., Heys, D. R., & Heys, R. J. (1977). A gravity perfusion technique for lab animals. *Laboratory Animals*, *6*, 18–22.

Desjardins, C., & Parent, A. (1992). Distribution of somatostatin immunoreactivity in the forebrain of the squirrel monkey: Basal ganglia and amygdala. *Neuroscience*, *47*, 115–133.

Fairén, A., & Valverde, F. (1980). A specialized type of neuron in the visual cortex of cat: A Golgi and electron microscope study of chandelier cells. *The Journal of Comparative Neurology*, *194*, 761–779.

Fox, C. A., Ubeda-Purkiss, M., Ihrig, K., & Biagioli, D. (1951). Zinc chromate modification of the Golgi technic. *Stain Technology*, *26*, 109–114.

Hall, E. (1972). The amygdala of the cat: A Golgi study. *Zeitschrift für Zellforschung*, *134*, 439–458.

Herzog, A. G. (1982). The relationship of dendritic branching complexity to ontogeny and cortical connectivity in the pyramidal cells of the monkey amygdala: A Golgi study. *Brain Research*, *256*, 73–77.

Jones, E. G. (1975). Varieties and distribution of non-pyramidal cells in the somatic sensory cortex of the squirrel monkey. *The Journal of Comparative Neurology*, *160*, 205–267.

Kamal, A. M., & Tömböl, T. (1975). Golgi studies on the amygdaloid nuclei of the cat. *Journal für Hirnforschung*, *16*, 175–201.

Kawaguchi, Y., & Kubota, Y. (1997). GABAergic cell subtypes and their synaptic connections in rat frontal cortex. *Cerebral Cortex*, *7*, 476–486.

Kemppainen, S., & Pitkänen, A. (2000). Distribution of parvalbumin, calretinin, and calbindin-D (28k) immunoreactivity in the rat amygdaloid complex and colocalization with gamma-aminobutyric acid. *The Journal of Comparative Neurology*, *426*, 441–467.

Kubota, Y., & Kawaguchi, Y. (1994). Three classes of GABAergic interneurons in neocortex and neostriatum. *The Japanese Journal of Physiology*, *44*(Suppl 2), S145–S148.

Kubota, Y., & Kawaguchi, Y. (1997). Two distinct subgroups of cholecystokinin-immunoreactive cortical interneurons. *Brain Research*, *752*, 175–183.

Lund, J. S. (1973). Organization of neurons in the visual cortex, area 17, of the monkey (*Macaca mulatta*). *The Journal of Comparative Neurology*, *147*, 455–496.

Mańko, M., Bienvenu, T. C., Dalezios, Y., & Capogna, M. (2012). Neurogliaform cells of amygdala: A source of slow phasic inhibition in the basolateral complex. *The Journal of Physiology*, *590*, 5611–5627.

Mascagni, F., & McDonald, A. J. (2003). Immunohistochemical characterization of cholecystokinin containing neurons in the rat basolateral amygdala. *Brain Research*, *976*, 171–184.

Mascagni, F., Muly, E. C., Rainnie, D. G., & McDonald, A. J. (2009). Immunohistochemical characterization of parvalbumin-containing interneurons in the monkey basolateral amygdala. *Neuroscience*, *158*, 1541–1550.

McDonald, A. J. (1982). Neurons of the lateral and basolateral amygdaloid nuclei: A Golgi study in the rat. *The Journal of Comparative Neurology*, *212*, 293–312.

McDonald, A. J. (1984). Neuronal organization of the lateral and basolateral amygdaloid nuclei in the rat. *The Journal of Comparative Neurology*, *222*, 589–606.

McDonald, A. J. (1985). Immunohistochemical identification of gamma-aminobutyric acid containing neurons in the rat basolateral amygdala. *Neuroscience Letters*, *53*, 203–207.

McDonald, A. J. (1987). Organization of amygdaloid projections to the mediodorsal thalamus and prefrontal cortex: A fluorescence retrograde transport study in the rat. *The Journal of Comparative Neurology*, *262*, 46–58.

McDonald, A. J. (1989). Coexistence of somatostatin with neuropeptide Y, but not with cholecystokinin or vasoactive intestinal peptide, in neurons of the rat amygdala. *Brain Research*, *500*, 37–45.

McDonald, A. J. (1992). Cell types and intrinsic connections of the amygdala. In J. P. Aggleton (Ed.), *The amygdala Neurobiological aspects of emotion, memory, and mental dysfunction* (pp. 67–96). New York: Wiley-Liss.

McDonald, A. J. (1994). Calretinin immunoreactive neurons in the basolateral amygdala of the rat and monkey. *Brain Research*, *667*, 238–242.

McDonald, A. J. (2019). Functional neuroanatomy of the basolateral amygdala: Neurons, neurotransmitters, and circuits. In J. Urban & A. Rosenkranz (Eds.), *Handbook of amygdala structure and function*. Amsterdam: Elsevier (In Press).

McDonald, A. J., & Augustine, J. R. (1993). Localization of GABA-like immunoreactivity in the monkey amygdala. *Neuroscience*, *52*, 281–294.

McDonald, A. J., & Betette, R. (2001). Parvalbumin containing neurons in the rat basolateral amygdala: Morphology and colocalization of calbindin D-28k. *Neuroscience*, *102*, 413–425.

McDonald, A. J., & Culberson, J. L. (1981). Neurons of the basolateral amygdala: A Golgi study in the opossum. *Amer. Journal of Anatomy*, *162*, 327–342.

McDonald, A. J., & Mascagni, F. (2001). Colocalization of calcium-binding proteins and gamma-aminobutyric acid in neurons of the rat basolateral amygdala. *Neuroscience*, *105*, 681–693.

McDonald, A. J., & Mascagni, F. (2002). Immunohistochemical characterization of somatostatin containing interneurons in the rat basolateral amygdala. *Brain Research*, *943*, 237–244.

McDonald, A. J., & Mascagni, F. (2019). Cholecystokinin immunoreactive neurons in the basolateral amygdala of the rhesus monkey (*Macaca mulatta*). *The Journal of Comparative Neurology*, *527*, 2694–2702.

McDonald, A. J., Mascagni, F., & Augustine, J. R. (1995). Neuropeptide Y and somatostatin-like immunoreactivity in the monkey amygdala: Distribution, morphology, and differential coexistence. *Neuroscience*, *66*, 959–982.

McDonald, A. J., Mascagni, F., & Zaric, V. (2012). Subpopulations of somatostatin-immunoreactive non-pyramidal neurons in the amygdala and adjacent external capsule project to the basal forebrain: Evidence for the existence of GABAergic projection neurons in the cortical nuclei and basolateral nuclear complex. *Front Neural Circuits*, *6*, 46.

McDonald, A. J., & Zaric, V. (2015). GABAergic somatostatin-immunoreactive neurons in the amygdala project to the entorhinal cortex. *Neuroscience*, *290*, 227–242.

Millhouse, O. E., & DeOlmos, J. (1983). Neuronal configurations in lateral and basolateral amygdala. *Neuroscience*, *10*, 1269–1300.

Morest, D. K. (1981). The Golgi Methods. In C. Heym & W.-F. Forssmann (Eds.), *Techniques in neuroanatomical research* (pp. 124–138). Berlin, Germany: Springer-Verlag.

Morgan, J. T., & Amaral, D. G. (2014). Comparative analysis of the dendritic organization of principal neurons in the lateral and central nuclei of the rhesus macaque and rat amygdala. *The Journal of Comparative Neurology*, *522*, 689–716.

Mukhina, Y. K., & Leontovich, T. A. (1970). Neuronal structure of some amygdaloid nuclei in dogs. *Arkhiv Anatomii Gistologii i Embriologii*, *59*, 62–70.

Muller, J. F., Mascagni, F., & McDonald, A. J. (2003). Synaptic interconnections of distinct interneuronal subpopulations in the rat basolateral amygdalar nucleus. *The Journal of Comparative Neurology*, *456*, 217–236.

Muller, J. F., Mascagni, F., & McDonald, A. J. (2005). Coupled networks of parvalbumin-immunoreactive interneurons in the rat basolateral amygdala. *The Journal of Neuroscience*, *25*, 7366–7376.

Muller, J. F., Mascagni, F., & McDonald, A. J. (2006). Pyramidal cells of the rat basolateral amygdala: Synaptology and innervation by parvalbumin-immunoreactive interneurons. *The Journal of Comparative Neurology*, *494*, 635–650.

Muller, J. F., Mascagni, F., & McDonald, A. J. (2007). Postsynaptic targets of somatostatin-containing interneurons in the rat basolateral amygdala. *The Journal of Comparative Neurology*, *500*, 513–529.

Overstreet-Wadiche, L., & McBain, C. J. (2015). Neurogliaform cells in cortical circuits. *Nature Reviews. Neuroscience*, *16*, 458–468.

Oya, H., Kawasaki, H., Howard, M. A., 3rd, & Adolphs, R. (2002). Electrophysiological responses in the human amygdala discriminate emotion categories of complex visual stimuli. *The Journal of Neuroscience*, *22*, 9502–9512.

Pantazopoulos, H., Lange, N., Hassinger, L., & Berretta, S. (2006). Subpopulations of neurons expressing parvalbumin in the human amygdala. *The Journal of Comparative Neurology*, *496*, 706–722.

Pape, H. C., & Paré, D. (2010). Plastic synaptic networks of the amygdala for the acquisition, expression, and extinction of conditioned fear. *Physiological Reviews*, *90*, 419–463.

Paré, D., & Collins, D. R. (2000). Neuronal correlates of fear in the lateral amygdala: Multiple extracellular recordings in conscious cats. *The Journal of Neuroscience*, *20*, 2701–2710.

Paré, D., Collins, D. R., & Pelletier, J. G. (2002). Amygdala oscillations and the consolidation of emotional memories. *Trends in Cognitive Sciences*, *6*, 306–314.

Peters, A., & Proskauer, C. C. (1980). Smooth or sparsely spined cells with myelinated axons in rat visual cortex. *Neuroscience*, *5*, 2079–2092.

Pitkänen, A., & Amaral, D. G. (1993a). Distribution of parvalbumin-immunoreactive cells and fibers in the monkey temporal lobe: The amygdaloid complex. *The Journal of Comparative Neurology*, *331*, 14–36.

Pitkänen, A., & Amaral, D. G. (1993b). Distribution of calbindin-D28k immunoreactivity in the monkey temporal lobe: The amygdaloid complex. *The Journal of Comparative Neurology*, *331*, 199–224.

Pitkänen, A., & Amaral, D. G. (1994). The distribution of GABAergic cells, fibers, and terminals in the monkey amygdaloid complex: An immunohistochemical and in situ hybridization study. *The Journal of Neuroscience*, *14*, 2200–2224.

Prager, E. M., Bergstrom, H. C., Wynn, G. H., & Braga, M. F. (2016). The basolateral amygdala γ-aminobutyric acidergic system in health and disease. *Journal of Neuroscience Research*, *94*, 548–567.

Price, C. J., Cauli, B., Kovacs, E. R., Kulik, A., Lambolez, B., Shigemoto, R., & Capogna, M. (2005). Neurogliaform neurons form a novel inhibitory network in the hippocampal CA1 area. *The Journal of Neuroscience*, *25*, 6775–6786.

Price, J. L., & Slotnick, B. M. (1983). Dual olfactory representation in the rat thalamus: An anatomical and electrophysiological study. *The Journal of Comparative Neurology*, *215*, 63–77.

Ramón-Moliner, E. (1967). A source of error in the study of Golgi-stained material. *Archives Italiennes de Biologie*, *105*, 139–148.

Rhomberg, T., Rovira-Esteban, L., Vikór, A., Paradiso, E., Kremser, C., Nagy-Pál, P., … Hájos, N. (2018). VIP-immunoreactive interneurons within circuits of the mouse basolateral amygdala. *The Journal of Neuroscience*, *38*, 6983–7003.

Równiak, M., Szteyn, S., & Robak, A. (2003). A comparative study of the mammalian amygdala: A Golgi study of the basolateral amygdala. *Folia Morphologica*, *62*, 331–339.

Russchen, F. T., Amaral, D. G., & Price, J. L. (1987). The afferent input to the magnocellular division of the mediodorsal thalamic nucleus in the monkey, *Macaca fascicularis*. *The Journal of Comparative Neurology*, *256*, 175–210.

Schwartzberg, M., Unger, J., Weindl, A., & Lange, W. (1990). Distribution of neuropeptide Y in the prosencephalon of man and cotton-head tamarin (*Saguinus oedipus*): Colocalization with somatostatin in neurons of striatum and amygdala. *Anat Embryol (Berl).*, *181*, 157–166.

Seidenbecher, T., Laxmi, T. R., Stork, O., & Pape, H. C. (2003). Amygdalar and hippocampal theta rhythm synchronization during fear memory retrieval. *Science*, *301*, 846–850.

Simon, A., Oláh, S., Molnár, G., Szabadics, J., & Tamás, G. (2005). Gap-junctional coupling between neurogliaform cells and various interneuron types in the neocortex. *The Journal of Neuroscience*, *5*, 6278–6285.

Somogyi, P. (1977). A specific 'axo-axonal' interneuron in the visual cortex of the rat. *Brain Research*, *136*, 345–350.

Sorvari, H., Soininen, H., Paljärvi, L., Karkola, K., & Pitkänen, A. (1995). Distribution of parvalbumin-immunoreactive cells and fibers in the human amygdaloid complex. *The Journal of Comparative Neurology*, *360*, 185–212.

Sorvari, H., Soininen, H., & Pitkänen, A. (1996a). Calretinin-immunoreactive cells and fibers in the human amygdaloid complex. *The Journal of Comparative Neurology*, *369*, 188–208.

Sorvari, H., Soininen, H., & Pitkänen, A. (1996b). Calbindin-D28K-immunoreactive cells and fibres in the human amygdaloid complex. *Neuroscience*, *75*, 421–443.

Spampanato, J., Polepalli, J., & Sah, P. (2011). Interneurons in the basolateral amygdala. *Neuropharmacology*, *60*, 765–773.

Timbie, C., & Barbas, H. (2015). Pathways for emotions: Specializations in the amygdalar, mediodorsal thalamic, and posterior orbitofrontal network. *The Journal of Neuroscience*, *35*, 11976–11987.

Tömböl, T., & Szafrańska-Kosmal, A. (1972). A golgi study of the amygdaloid complex in the cat. *Acta Neurobiologiae Experimentalis (Wars)*, *32*, 835–848.

Tosevski, J., Malikovic, A., Mojsilovic-Petrovic, J., Lackovic, V., Peulic, M., Sazdanovic, P., & Alexopulos, C. (2002). Types of neurons and some dendritic patterns of basolateral amygdala in humans—A golgi study. *Annals of Anatomy*, *184*, 93–103.

Vereczki, V. K., Veres, J. M., Müller, K., Nagy, G. A., Rácz, B., Barsy, B., & Hájos, N. (2016). Synaptic organization of perisomatic GABAergic inputs onto the principal cells of the mouse basolateral amygdala. *Frontiers in Neuroanatomy*, *10*, 20.

Veres, J. M., Nagy, G. A., & Hájos, N. (2017). Perisomatic GABAergic synapses of basket cells effectively control principal neuron activity in amygdala networks. *eLife*, *6*, e20721.

Veres, J. M., Nagy, G. A., Vereczki, V. K., Andrási, T., & Hájos, N. (2014). Strategically positioned inhibitory synapses of axo-axonic cells potently control principal neuron spiking in the basolateral amygdala. *The Journal of Neuroscience*, *34*, 16194–161206.

Wolff, S. B., Gründemann, J., Tovote, P., Krabbe, S., Jacobson, G. A., Müller, C., ... Lüthi, A. (2014). Amygdala interneuron subtypes control fear learning through disinhibition. *Nature*, *509*, 453–458.

Woodruff, A. R., & Sah, P. (2007). Networks of parvalbumin-positive interneurons in the basolateral amygdala. *The Journal of Neuroscience*, *27*, 553–563.